ACS APPLIED MATERIALS & INTERFACES

Research Article

www.acsami.org

# Using in-Situ Polymerization of Conductive Polymers to Enhance the Electrical Properties of Solution-Processed Carbon Nanotube Films and Fibers

Ranulfo Allen,[†] Lijia Pan,[‡] Gerald G. Fuller,[†] and Zhenan Bao*[,†]

[†]Department of Chemical Engineering, Stanford University, Stanford, California 94305-5025, United States

[‡]National Laboratory of Microstructures (Nanjing), School of Electronic Science and Engineering, Nanjing University, Nanjing 210093, China

Supporting Information

**ABSTRACT:** Single-walled carbon nanotubes/polymer composites typically have limited conductivity due to a low concentration of nanotubes and the insulating nature of the polymers used. Here we combined a method to align carbon nanotubes with in-situ polymerization of conductive polymer to form composite films and fibers. Use of the conducting polymer raised the conductivity of the films by 2 orders of magnitude. On the other hand, CNT fiber formation was made possible with in-situ polymerization to provide more mechanical support to the CNTs from the formed conducting polymer. The carbon nanotube/conductive polymer composite films and fibers had conductivities of 3300 and 170 S/cm, respectively. The relatively high conductivities were attributed to the polymerization process, which doped both the SWNTs and the polymer. In-situ polymerization can be a promising solution-processable method to enhance the conductivity of carbon nanotube films and fibers.

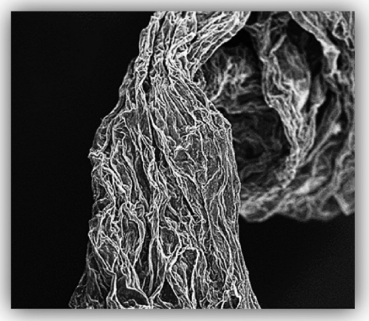

**KEYWORDS:** *carbon nanotube fibers, carbon nanotube thin films, conductive polymer composites, PEDOT, solution processing, carbon nanotube alignment*

In recent decades, electronic skins and wearable devices have received intense interest.[1−3] Development of these devices calls for research on highly conducting thin films and weavable fibers. Carbon nanotubes (CNTs), a strong candidate from a materials consideration, have remarkable mechanical and electrical properties. This has led to their applications in polymer reinforcement and as electrodes and fibers. CNT thin films have been explored as transparent, conductive electrodes.[4−8] Carbon nanotube fibers have been explored since they expand the applications beyond those found for carbon fibers, which are only used in applications that demand lightweight, high-strength materials. CNT fibers may also find applications in supercapacitors[9−11] and muscle actuators.[12,13] Various methods have been used to form CNT fibers, such as spinning from CNT forests,[14,15] spinning from CNT aerogels,[16] twisting from CNT thin films,[17] gel spinning,[18] electrospinning,[19] and wet spinning.[20,21]Chou et al. recently reviewed these techniques.[22] However, in general there are two methods to spin nanosized CNTs into macroscopic long fibers: using ultralong CNTs with lengths on the order of centimeters[14] or using a polymer binder to adhere short and small CNTs into a macroscopic fiber.[23] However, the former method needs ultralong CNTs that are expensive and not commercially available in large scale. Most of the works related to the latter method used insulating polymer as binders that greatly reduced the conductivity of CNTs fibers.

Herein, we proposed a novel method that used in-situ-polymerized conducting polymer to aid in solidifying a single-walled carbon nanotube (SWNT) dispersed gel with a low yield stress to form a SWNT/conjugated polymer composite film or fiber. This method involves solution processes that are amenable to large-area, roll-to-roll films or continuous fiber production. Our results showed that the produced SWNT/conjugated polymer composite thin film and fibers were composed of well-aligned carbon nanotubes, which were aligned under shearing forces during blading and extruding. This alignment was similar to our findings in previous studies.[24,25] The carbon nanotube/conductive polymer composite films and fibers exhibited high conductivities of 170 and 3300 S/cm, respectively. Further investigation by absorption and Raman spectra indicated that both the polymers and the carbon nanotubes were doped, which resulted in high conductivities. Our in-situ polymerization of conducting polymer can be a general solution-processable method to promote production and conductivity of CNT films and fibers. A detailed comparison between various methods to form carbon nanotube fibers highlighting the advantages of this solution-processable method is presented in the Results and Discussion section.

## MATERIALS AND METHODS

Arc-discharged single-walled carbon nanotubes (SWNT, ASP-100F) were purchased from Hanwha Nanotech Corp., Korea. The nanotubes

Received: September 2, 2013
Accepted: June 10, 2014
Published: June 10, 2014

   dx.doi.org/10.1021/am5019995 | ACS Appl. Mater. Interfaces 2014, 6, 9966−9974

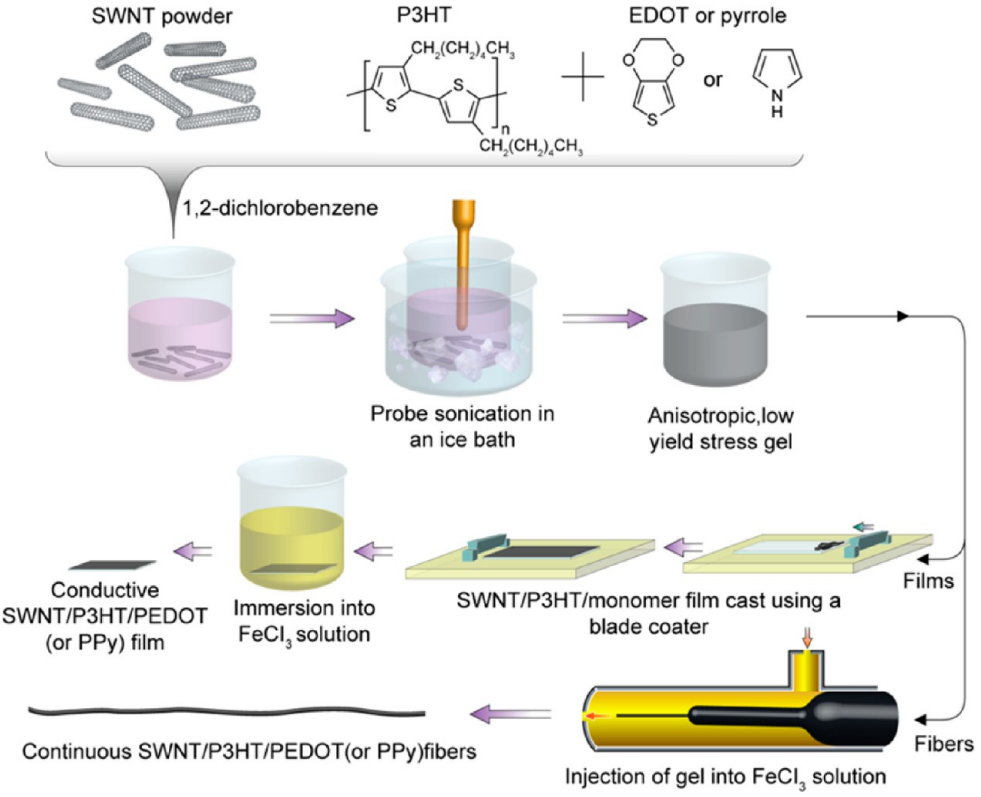


**Figure 1.** Scheme illustrating the method to use in-situ polymerization to form conductive films and fibers.

had an average diameter of about 1.4 nm. All other materials were purchased from Sigma-Aldrich (US) unless otherwise specified. Regioregular poly(3-hexyl thiophene) (P3HT) was used to disperse and align the nanotubes. All chemicals were used as received. No further purification of the materials was carried out. The composite dispersions were made by adding the appropriate amounts of polymer and CNT into a small vial so as to have a 1 to 1 weight ratio. 1,2-Dichlorobenzene (oDCB) was then added to make a 2 mg SWNT/mL dispersion. Note that our past studies involved varying the ratio of SWNT to polymer as well as the choice of solvent and polymer.[25] It was found that this particular dispersion led to the greatest level of gel-like properties and alignment of SWNTs. The dispersion was then sonicated using a Cole-Palmer Ultrasonicator at 300 W for 15 min in an ice bath. After sonication at the above conditions, the average CNT length was about 1.5 $\mu$m. Note that no further centrifugation or purification was carried out after sonication due to the good uniform dispersion as previously reported.[26] For films and fibers with in-situ polymerization of conductive polymer, the corresponding monomer, pyrrole (Py) or 3,4-ethylenedioxythiophene (EDOT) (Fisher Scientific, US), was then added to the dispersion at a 40/1 (monomer/CNT) weight ratio. Anhydrous iron(III) chloride was added to anhydrous ethanol at a 0.5 M concentration. Phytic acid dodecasodium salt (Fisher Scientific, US) was added to some ferric chloride solutions at a 50/1 $FeCl_3$/phytic acid molar ratio.

Figure 1 schematically illustrated the process using in-situ-polymerized conducting polymers to form SWNT/P3HT/PPy or SWNT/P3HT/PEDOT films and fibers. The SWNT/P3HT/monomer dispersions were prepared. Then the dispersion was coated onto a glass slide into a film or extruded from a syringe to form fibers. The SWNT film and fibers were brought to contact with iron(III) chloride. $FeCl_3$ initiated polymerization of the conducting polymer, which formed a film on the SWNT films and aided to solidify the SWNT fibers. Phytic acid was added to the oxidizing solution for certain tests to cross-link the PPy and PEDOT.

Films were made using a motorized film applicator with a Bird attachment (Elcometer, UK). Films were cast at 100 mm/s with a 20 $\mu$m gap onto glass slides. A thin wet film was produced. For some samples, this wet film was immersed into the ferric chloride solution. These samples were labeled "wet". For other samples, the solvent was evaporated at room temperature. Once dried, these films were placed into the ferric chloride solution to induce polymerization of the conjugated polymer. These samples were labeled "dry". After 5 min in the $FeCl_3$ solution, the glass slide was immersed and gently shook in ethanol to remove excess $FeCl_3$. They were then dried in air.

Potentially continuous fibers were formed by flowing the ethanol solution with the SWNT/P3HT/Py dispersion in oDCB using a peristaltic pump and a syringe pump, respectively. The average fluid velocity of the ethanol solution was 65 mm/s. The SWNT dispersion was flowed into the center of the tubing at an average velocity of 15 mm/s. For a 30 gauge needle and 18 gauge tubing, these velocities correspond to flow rates of 4.67 and 0.036 mL/min, respectively. Teflon tubing and blunt Teflon needles were used for continuous production. Various tubing and needle sizes were used, and the flow rates were modified to maintain these velocities. The ratio of the inner diameters of the needle and tubing was maintained at about 8. The SWNT/P3HT/Py and $FeCl_3$ velocities were kept at 3 and 6.5 cm/s, respectively. Initial tests used a 30 gauge Teflon needle with 18 gauge Teflon tubing. The tubing length was about 2 m. For these tests the $FeCl_3$ solution was kept in a freezer and the SWNT/P3HT/Py dispersion was kept in a refrigerator until use to lower the reaction temperature to promote the exothermic reaction.

Films and fibers were imaged using a FEI XL30 Sirion Scanning Electron Microscope (SEM). Some fibers were cut using tweezers or scissors to image the breakage of the fibers. A two-point probe was used to measure the resistance of at least three fibers with varying lengths for each parameter set. By measuring varying lengths of each fiber, a resistance per length was calculated. Silver paint was used as the electrode contacts. The conductivity was calculated from the resistance measurements and the diameters of the fibers as determined from SEM images. A four-point probe with 5 mm spacing was used to measure the sheet resistance for films. The sheet resistance of the films was calculated using equations incorporating the geometry of a thin, narrow, rectangular sample.[27−29] The conductivity was calculated from these measurements using thickness measurements from a profilometer

(Veeco Dektak 150). Films were further characterized using absorption spectroscopy (Varian Cary6000i) and Raman spectroscopy (Horiba LabRam ARAMIS using a 633 nm laser). Transmittance values are given at 550 nm.

## RESULTS AND DISCUSSION

**SWNT/P3HT/PPy and SWNT/P3HT/PEDOT Films.** We previously reported that single-walled carbon nanotube/regioregular poly(3-hexyl thiophene) (SWNT/P3HT) dispersions in oDCB can form gels that contain aligned domains similar to liquid crystal solutions.[25] Under a shear force, these domains can be aligned along the shearing direction. We previously investigated this alignment and its effect on transparent electrode performance.[24] However, SWNT films conductive enough for use as transparent electrodes required removal of the dispersant polymer using high temperatures. Even though the P3HT dispersing polymer was conjugated, it is insulating and hindered the performance of the films when it was undoped. This prevented use of plastic substrates or required a transfer process. An alternative approach is to enhance the conductivity of SWNT/P3HT films by doping or adding a conductive material like a conductive polymer. In-situ polymerization of polypyrrole or PEDOT was done to enhance the conductivity. This is illustrated in Figure 1. The respective monomers, either pyrrole or EDOT, were added to the SWNT/P3HT dispersion. The weight ratio was varied to form a 1/1/4, 1/1/40, or 1/1/400 (SWNT/P3HT/monomer) dispersion. The 1/1/400 dispersion was not stable as this amount of monomer destabilized the SWNT dispersion. Films were made using a Bird film applicator with an automated shearing table. The shear speed for depositing these films was 100 mm/s with a 20 $\mu$m gap. This produced a wet SWNT/P3HT/Py film. For some samples, this wet film was then placed into a 0.5 M $FeCl_3$ ethanol solution. These samples are labeled "wet". For others, the dichlorobenzene was allowed to evaporate to lead to a dried film before immersion into the $FeCl_3$ solution. These samples are labeled "dry". PPy or PEDOT was formed after exposure to $FeCl_3$ to create a thin SWNT/P3HT/PPy or SWNT/P3HT/PEDOT film.

Without addition of the conductive polymer, a SWNT/P3HT film had a sheet resistance of 20 kΩ/□ at 81% transmittance. A popular benchmark for comparing transparent electrodes is to use the DC to optical conductivity ratio ($D/O$).[30] The corresponding DC to optical conductivity ratio for the SWNT/P3HT film was 0.08. When this film was doped with $FeCl_3$, a known dopant for SWNTs and conjugated polymers, it had a 500 Ω/□ sheet resistance at 88% transmittance corresponding to a 5.64 D/O, a 2 orders of magnitude increase. Films with addition of conductive polymer showed a further increase in conductivity, reaching a $D/O$ of 11. Compared to the SWNT/P3HT films, this is an increase in transparent electrode performance of 2 orders of magnitude. Those films made under a wet polymerization were less conductive than the dried films. The dried films had a 93 Ω/□ sheet resistance at 68% transmittance compared to 290 Ω/□ at 83% transmittance for the wet films. These corresponded to DC to optical conductivity ratios of 9.6 and 6.5, respectively. The conductive polymer enhanced the electrical performance of these films more than doping with $FeCl_3$. SEM images of SWNT/P3HT/PPy films are shown in Figure 2. A representative SWNT/P3HT film with no additional polymer is shown in Figure 2A. The multiple layers of SWNTs were partially aligned. Addition of PPy did not change the morphology of the film drastically. The CNTs remained partially aligned but appeared wrapped with a thin PPy coating. The PPy coating was rougher in the film that was polymerized before evaporation of the oDCB, and this could account for the decreased conductivities for the wet films. Films with PEDOT appeared very similar to these images and are shown in Figure S1, Supporting Information. The conductivities of the films are shown in Table 1.

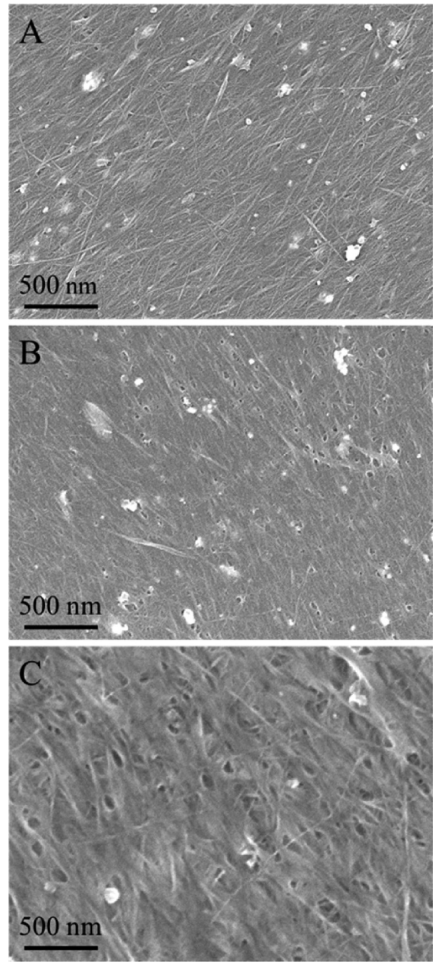


**Figure 2.** SEM images of SWNT/conjugated polymer films. (A) SWNT/P3HT (1/1) film as cast. (B) SWNT/P3HT/PPy film as cast. SWNT/P3HT/Py (1/1/40) was allowed to dry before polymerization of the PPy. (C) SWNT/P3HT/PPy film as cast. SWNT/P3HT/Py (1/1/40) film was immersed into $FeCl_3$ before solvent evaporation could occur. Scale bars are 500 nm.

Absorption and Raman spectroscopies were used to probe the doping of the conjugated polymers and SWNTs. Figure 3A shows the absorption spectra for a SWNT/P3HT film before and after immersion into a ferric chloride solution for 5 min. The P3HT absorption peak at 570 nm dropped substantially while a new peak appeared at 800 nm due to doped polythiophene.[31,32] In addition, the CNT peak at 1000 nm shifted slightly and could not be distinguished from the 800 nm peak. With the appearance of a peak at 800 nm, the polythiophene wrapping the nanotubes appeared to be doped. The corresponding Raman spectra are shown in Figure 3B. The intensity of the polymer peak at 1440 $cm^{-1}$ was diminished, and the shape of the G band of the carbon nanotubes sharpened and shifted slightly to a higher wavenumber by about 1.5 $cm^{-1}$, indicating p doping of the SWNTs. Doping of both the SWNTs


dx.doi.org/10.1021/am5019995 | ACS Appl. Mater. Interfaces 2014, 6, 9966−9974

**Table 1. Raman Peak Shifts (in $cm^{-1}$) and Transparent Electrode Performance for Various SWNT-Conjugated Polymer Films**

| film | CNT $G^+$ upshift ($cm^{-1}$) | average $R_S$ ($\Omega/\square$) | %$T$ at 550 nm | $\sigma_{DC}/\sigma_{optical}$ | conductivity (S/cm) |
|---|---|---|---|---|---|
| SWNT/P3HT doped | 1.52 | 500 | 88 | 5.6 | 1300 |
| SWNT/P3HT/PPy 1/1/4 dry[a] | 3.14 | 240 | 88 | 11 | 1700 |
| SWNT/P3HT/PPy 1/1/40 dry | 4.88 | 93 | 68 | 9.6 | 2800 |
| SWNT/P3HT/PPy 1/1/40 wet[b] | 9.75 | 290 | 83 | 6.5 | 1000 |
| SWNT/P3HT/ PEDOT 1/1/4 dry | 3.68 | 170 | 82 | 11 | 2100 |
| SWNT/P3HT/ PEDOT 1/1/40 dry | 4.66 | 85 | 71 | 12 | 3300 |
| SWNT/P3HT/ PEDOT 1/1/40 wet | 7.37 | 340 | 79 | 4.4 | 770 |

[a]Solvent was evaporated before immersion into ferric chloride solution. [b]Solvent was not evaporated before immersion into ferric chloride solution.

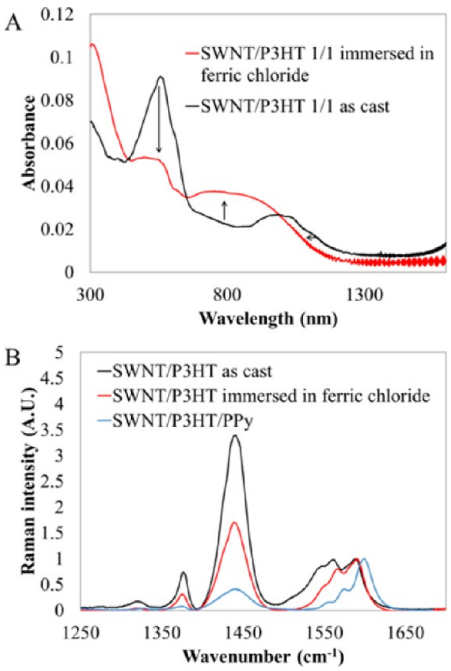


**Figure 3.** (A) Absorption spectra for SWNT/P3HT films. Upon immersion in ferric chloride, the polymer peak at 570 nm decreased while the peak corresponding to doped P3HT at 800 nm rose. (B) Raman spectra for SWNT/P3HT films. Upon immersion in ferric chloride, the polymer peaks dropped in intensity while the G band hardened and slightly upshifted. A SWNT/P3HT/PPy film had a greater upshift.

and P3HT accounted for the decrease in sheet resistance from 20 000 to 500 $\Omega/\square$ after immersion in $FeCl_3$. The spectrum for a SWNT/P3HT/PPy film is also shown in Figure 3B. The G-band shift is even greater by 8.2 $cm^{-1}$, indicating a greater level of p doping compared to the $FeCl_3$-doped SWNT/P3HT film.

The level of doping for the various films made with varying processing conditions was monitored by shifts in the Raman spectra and changes in the absorption spectra. Using a SWNT/P3HT as cast film as a control, shifts in the CNT $G^+$ peak are tabulated in Table 1 for several SWNT/conjugated polymer films. The largest shifts were found to occur when the film was still wet when immersed into the ferric chloride solution to polymerize the conductive polymer. These processing conditions resembled that to be used for producing fibers. However, these highly doped films did not lead to the most conductive films as shown in Table 1. The optimal conditions for high conductivity involved allowing the oDCB to evaporate before immersion into the ferric chloride. A 1/1/40 (SWNT/P3HT/monomer) weight ratio yielded the best results. Conductivities of 2800 and 3300 S/cm have been reached for SWNT/P3HT/PPy and SWNT/P3HT/PEDOT films, respectively. Other solution-processed films require strong acidic dopants, which prevent universal use in flexible electronics. This is the first use of industrial deposition methods to solution-process conductive carbon nanotube composite films uniformly over large areas.

**SWNT/P3HT/PPy and SWNT/P3HT/PEDOT Fibers.** These low-yield stress, gelated SWNT/P3HT dispersions should allow for fibers with aligned carbon nanotubes. We can take advantage of the gel-like properties of the dispersions so that the dispersion maintains its cylindrical shape when injected into a second medium, resulting in a gel fiber. One would suspect that the solvent could be removed from the gel fibers through diffusion into a second medium, be it air or a miscible solvent. This would result in a solid SWNT/P3HT fiber. However, we found that the gel fibers were too fragile to be processed via oDCB evaporation, and no solvent allowed for complete solidification of the gel fiber. More details on the coagulant solvents that were attempted are in the Supporting Information. Since the fibers did not solidify over time, another method had to be used to strengthen the gel fibers so that they could be processed.

Adding another component to these gel fibers to strengthen the gel state was thus necessary. We excluded insulating materials as they could diffuse in between the SWNTs and lower the conductivity. Conductive polymers were attractive candidates as they could help to hold nanotubes together while enhancing the overall conductivity of the fibers. Oxidation polymerization of pyrrole or EDOT could be carried out upon exposure of the monomer to the oxidizing ferric chloride. Similar to the SWNT/conjugated polymer films, ferric chloride would dope the polymers and the SWNTs to further enhance the overall conductivity.[33,34] Thus, formation of conductive polymer could stabilize and dope the fiber in one step. One major concern with conjugated polymers was the brittle nature commonly associated with thick, doped conjugated polymer films.[35−38] The brittleness is strongly related to the microstructure of the polymer coating; thus, optimization and sometimes addition of cross-linkers are needed to form a strong film.[36] Figure 1 illustrates the in-situ polymerization process used to form conductive films and fibers.

The in-situ polymerization process for the SWNT/P3HT films was adapted for processing fibers to allow for conductive, solid fibers. The in-situ polymerization during fiber processing closely resembles that of the "wet" films described earlier. Monomer was added to the SWNT/P3HT dispersions to form a 1/1/4 or a 1/1/40 (SWNT/P3HT/monomer) dispersion. The SWNT/P3HT/monomer dispersion was injected into a ferric chloride oxidizing solution. After injection, the monomer would undergo oxidation polymerization to form PPy or PEDOT. Several parameters had to be optimized to form fibers. These parameters included the flow rate of the SWNT/P3HT/Py dispersion, the injection needle size, the monomer concentration, the oxidant solution and concentration, and the drying

condition. Fibers without carbon nanotubes were also attempted using P3HT/Py solutions and 0.5 and 5 M $FeCl_3$, but no fibers could be formed in either case, indicating that the presence of SWNTs strengthened the polymer to allow formation of the observed fibers.

Infinitely long fibers could be formed by continuously flowing a $FeCl_3$ ethanol solution with the SWNT/P3HT/monomer oDCB dispersion. This process is shown in Figure 1. The $FeCl_3$ solution was pumped using a peristaltic pump into a T junction. The SWNT/P3HT/Py dispersion was pumped using a syringe pump past the T junction using a long Teflon needle. Thus, when the dispersion exited the needle it would flow coaxially with the $FeCl_3$ solution. Teflon tubing and needles were used to prevent any clogging. The tubing length after the end of the needle was controlled to vary the residence time of the fibers. Longer tubing lengths allowed for longer polymerization times. Fibers were collected in a large shallow dish. A shallow dish was needed as the fibers were very sensitive to static electricity, most likely due to the polymers being in a charged state. If the wet fiber adsorbed onto a surface, a film rather than a fiber would form. Fibers were slowly removed from this dish and allowed to dry in air to form solid fibers. The variables in this system included the flow rates of the two solutions, needle and tubing sizes, tubing length, and concentrations of the solutions. Initial conditions used were similar to those used by Davis et al.[21]

Optimization of this process is detailed in the Supporting Information. The narrowest needle size that was tested was optimal since it allowed a thin layer of conductive polymer to stabilize the fiber. With larger needles, the fibers would break up immediately after injection. We attributed this to the larger cross-sectional area of the fibers when using larger needles. More PPy must form to stabilize these thicker fibers due to the increased cross-sectional area. The monomer concentration needed to be great enough to lead to a sufficiently thick conductive polymer layer for stabilization of the fiber but not too great to induce SWNT precipitation. Varying the SWNT/P3HT/monomer dispersion velocity led to two regimes. For SWNT/P3HT/monomer velocities greater than the ferric chloride velocity, thick, coiled fibers of regular length were produced. The length of these fibers could be increased by increasing the SWNT/P3HT/monomer flow rate though continuous fibers could not be formed. Thin, straight, semicontinuous fibers could be produced by lowering the SWNT/P3HT/monomer flow rate well below the ferric chloride flow rate. An average velocity of 1.5 cm/s (0.018 mL/min flow rate) with a 6.5 cm/s $FeCl_3$ solution velocity produced these fibers. These semicontinuous fibers were several feet long but could not be dried without breakage due to their fragility. This prevented quantitative characterization of the mechanical properties of these fibers. Optical images of these two types of fibers are shown in Figure S9, Supporting Information.

SEM images of these fibers are shown in Figures 4 and 5. Thick, coiled fibers are shown in Figure 4. The diameters of the fibers were about 70 $\mu$m. The fiber structure was very rough with many wrinkles on the surface. The fibers had a large surface area due to these wrinkles. Nanotubes were observed to be within a PPy/PEDOT matrix with many PPy/PEDOT fibers on the surface, as shown in Figure 4B and 4E, respectively. The nanotubes appeared aligned along the folds in the fiber. The fiber had wrinkles within it that seemed to consist of nanofibers of about 30 nm in diameter as seen in Figure 4C and 4F. These nanofibers seemed to have a preferred orientation parallel

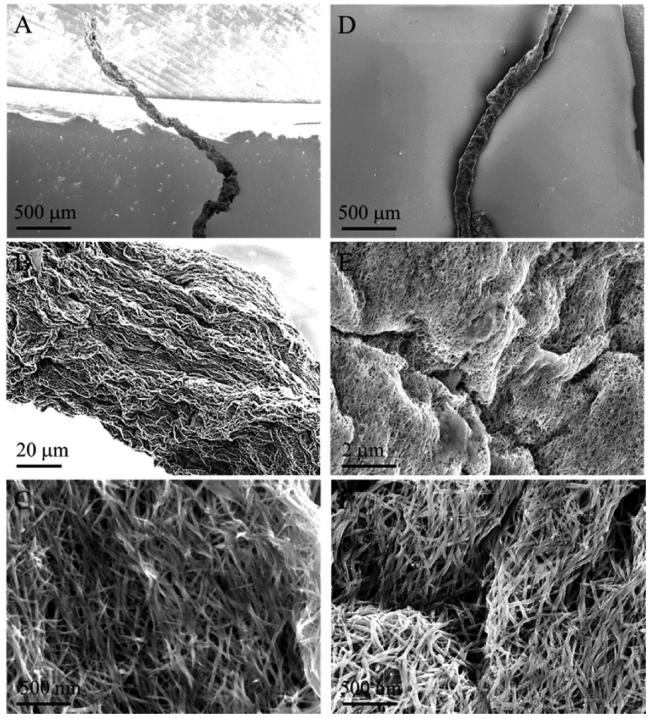


**Figure 4.** (A–C) SEM images of thick, coiled SWNT/P3HT/PPy fibers. (D–F) SEM images of SWNT/P3HT/PEDOT fibers. Fibers were formed by flowing SWNT/P3HT/monomer (1/1/40 weight ratio) with a 0.5 M $FeCl_3$ ethanol solution. Both types of fibers have similar morphologies. Polymerization was not uniform, leading to regions with a collapsed structure as shown in A and D. A rough PPy or PEDOT coating with many wrinkles was observed throughout the fiber. Conductive polymer nanofibers with diameters of about 30 nm were found among small CNT bundles in C and F.

to the fiber orientation. It was difficult to determine if these nanofibers consisted of only conjugated polymer or a mix with carbon nanotubes. These fibers were mechanically weak, leading to brittle fracture. A series of two-point probe resistance measurements for several fibers of various lengths revealed these fibers to have a conductivity of about 6 and 7 S/cm for SWNT/P3HT/PPy and SWNT/P3HT/PEDOT fibers, respectively. Though this conductivity was not high, the large surface area could be of interest for certain applications, such as supercapacitors.

Figure 5 shows SEM images of the semicontinuous fibers at different locations along the fiber. The diameter was about 22 $\mu$m. The fibers were rigid, with a straight orientation. The surface was much smoother than the thicker fibers, but folds were still prominent. These likely occurred during the drying process when the diameter of the fiber shrank. Slight cracks in the PPy coating could be observed as in Figure 5C. Figure 5D–F shows the fibers after fracture. Brittle fracture occurred as shown by the clean break. PPy could be observed throughout the fiber. Aligned CNTs could be seen protruding from the edge. No voids in the fiber were observed. The conductivity of these fibers was measured to be 170 S/cm. The smoother PPy films and improved PPy embedding into the CNTs may account for this increased conductivity. Though these fibers were conductive, the weak mechanical properties had to be improved to make these fibers practical. In addition, reproducibility of these fibers was low. A microfluidic device, which would provide more control, may be needed to consistently form these fibers.

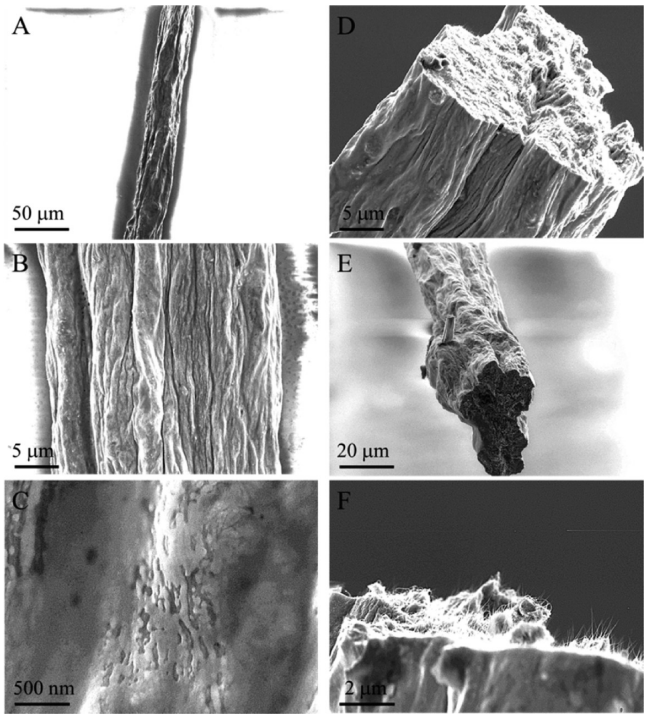


**Figure 5.** SEM images of semicontinuous SWNT/P3HT/PPy fibers. Fibers were formed by flowing SWNT/P3HT/Py (1/1/40 weight ratio) with a 0.5 M $FeCl_3$ ethanol solution. (A–C) Images of intact fibers. A smooth PPy coating with small cracks was observed throughout the fiber. (D–F) Images of the fibers after being cut with scissors. PPy could be seen to be well incorporated within the fiber. Aligned CNTs protruded from the edge.

**Strengthening Mechanical Properties of SWNT/P3HT Fibers.** To enhance the reproducibility and strength of these fibers, three strategies were employed: increasing the residence time, increasing the $FeCl_3$ concentration, and using phytic acid as a noncovalent cross-linker. Increasing the polymerization time may increase the yield for PPy. However, increasing the tubing length from 6 to 100 feet, which increased the residence time from 1 mi to about 15 min, did not improve the strength of the fibers. Increasing the $FeCl_3$ concentration increased the polymerization rate. The 0.05, 0.5, and 5 M $FeCl_3$ ethanol solutions were tested. Use of 0.05 M $FeCl_3$ lowered the reaction rate such that only short fibers were produced. These fibers were noticeably weaker than short fibers produced using 0.5 M $FeCl_3$. Using 5 M $FeCl_3$ led to fast polymerization rates. The resulting fibers were much thicker, with diameters greater than the inner diameter of the needle. Two types of fibers were formed when using 5 M $FeCl_3$: coiled fibers produced at faster flow rates and straight fibers produced at slow flow rates. These fibers were similar to those produced with 0.5 M $FeCl_3$ but with much thicker coatings of conductive polymer. The conductivity of SWNT/P3HT/PPy coiled and straight fibers were 0.7 and 3 S/cm, respectively. Nonetheless, neither regime led to continuous fiber production likely due to the large cracks in the polymer coatings, as shown in SEM images in Figure S8, Supporting Information.

Phytic acid allowed for cross-linking of the conductive polymer through electrostatic interactions. It had been used to form hydrogels with polyaniline by interacting with the nitrogen on the backbones of the polymer.[39] Use of phytic acid cross-linking may help to improve the mechanical strength of the fibers and produce continuous fibers more consistently. Since phytic acid had limited solubility in dichlorobenzene, it was added to the ferric chloride ethanol solution at a 6.6 mg/mL concentration to have a 50/1 $FeCl_3$/phytic acid molar ratio, similar to the concentration used for preparing hydrogels in previous studies.[39] When used with SWNT/P3HT/Py (1/1/40), a semicontinuous coiled fiber could be formed in contrast to the SWNT/P3HT/PPy fiber without the phytic acid, indicating an increase in strength. Again, these fibers were several feet long but could not be dried effectively to prevent breakage. These semicontinuous fibers were formed with the $FeCl_3$ flow rate of 4.6 mL/min (6.4 cm/s) and extrusion rate of 0.36 mL/min (30 cm/s). Thin, straight continuous fibers could not be formed due to fiber breakage near the injection point. The coiled fibers are shown in Figure 6A–C. The diameters of

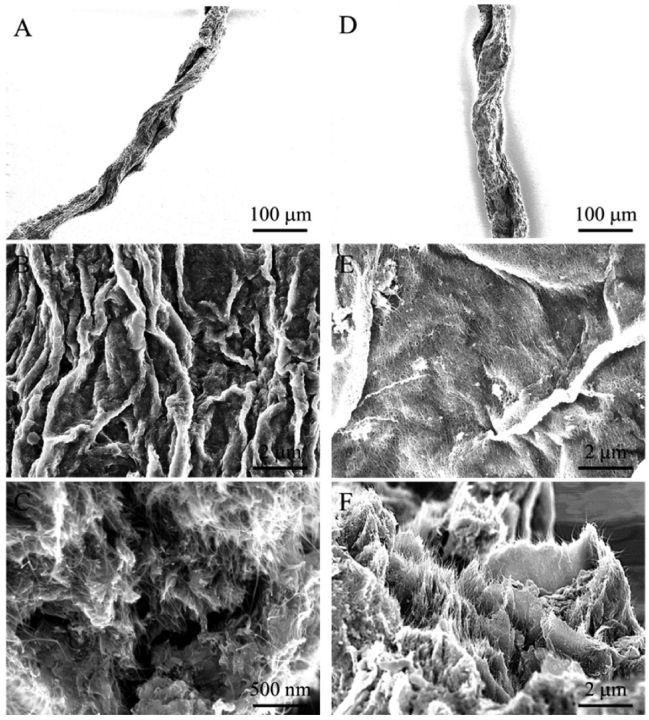


**Figure 6.** (A–C) SEM images of coiled SWNT/P3HT/PPy/phytic acid fibers. Fibers were formed by flowing SWNT/P3HT/PPy (1/1/40) with a 0.5 M $FeCl_3$ ethanol solution containing phytic acid. (A) The fiber was very coiled, with many portions of the fiber not being cylindrical. (B) Many wrinkles were observed (scale bar 2 μm). (C) Upon fracture, the layers within the fiber appeared broken at different points. (D–F) SEM images of coiled SWNT/P3HT/PEDOT/phytic acid fibers. Fibers were formed by flowing SWNT/P3HT/PEDOT (1/1/40) with a 0.5 M $FeCl_3$ ethanol solution containing phytic acid. (D) The fiber was coiled but still mainly cylindrical. (E) Fewer wrinkles were observed than in the PPy fiber. (F) Upon fracture, the layers within the fiber corresponded with the wrinkles found on the exterior of the fiber.

the fibers were about 46 μm. The fibers were not necessarily cylindrical, however, with some regions being flat. Similar to fibers without phytic acid, they had a large surface area due to the many folds and wrinkles found in these coiled fibers. These could be signs of a rapid drying process with a large change in the structure of the fiber. The PPy seemed to be well integrated within these folds. The end of a broken edge of a fiber is shown in Figure 6C. Brittle fracture and multiple layers were observed similar to other fibers. The multiple layers seemed to break


dx.doi.org/10.1021/am5019995 | ACS Appl. Mater. Interfaces 2014, 6, 9966–9974

independently, which could explain the weak, brittle nature of even these stronger fibers. The nanotubes appeared to be well dispersed in the layers and were aligned along the fiber orientation. No nanofibers were observed. This may explain the increase in conductivity up to 19 S/cm.

Phytic acid was also used with SWNT/P3HT/EDOT (1/1/40). Coiled, semicontinuous fibers were also formed. Optical images of these fibers are shown in Figure S10, Supporting Information. These fibers were more cylindrical showing that during the drying of the fiber the general shape was maintained as shown in Figure 6D−F. This could indicate a more uniform polymerization of PEDOT compared to PPy. This could be due to the lower oxidation potential of EDOT, which would allow PEDOT to form more easily around the gel fiber, allowing for a stronger cylindrical shell. The diameter of this fiber was 57 $\mu$m. Fewer wrinkles and folds were found in the fibers with PEDOT, though they were prevalent on the surface of the fiber. In Figure 6F these folds were observed to persist within the fiber, forming the layers that have been found in the other fibers. The conductivity of these fibers is 64 S/cm. The stronger interactions across polymer chains and lack of nanofibers may explain this increase in conductivity. SWNT/P3HT/PEDOT fibers with phytic acid were the strongest of all fibers produced as indicated by the ability to form semicontinuous fibers and the ease in removal from the ferric chloride solution without breakage. However, these fibers were still very brittle, likely due to poor interactions between the layers in the fiber. Thermogravimetric analysis was done for several fibers, and these data indicated that these SWNT/P3HT/PEDOT fibers with phytic acid contained the greatest carbon nanotube content. Details of this can be found in the Supporting Information.

In this work, several SWNT/conjugate polymer fibers were formed using in-situ polymerization of a conductive polymer. Note that no fibers were formed without addition of conductive polymer. All our fibers were relatively conductive, but past studies of these doped conductive polymers surpassed the conductivity of these fibers.[35,40] Compared to other solution-processed fibers using typical solvents, the conductivity of these SWNT/conjugated polymer fibers are promising. Vigolo et al. formed SWNT/poly(vinyl alcohol) (PVA) fibers by injecting surfactant-stabilized SWNT dispersions into an aqueous PVA solution.[23] The resulting fibers had a conductivity of 10 S/cm. Chen et al. formed similar fibers with a conductivity of 0.005 S/cm with the PVA and about 140 S/cm after annealing at 1000 °C in hydrogen to remove the PVA.[41] Foroughi et al. prepared MWNT/PPy fibers using MWNT forests and chemical polymerization leading to fibers with a conductivity of 270 S/cm compared to 215 S/cm without the PPy.[42] Compared to these studies, fibers up to 170 S/cm are on the same magnitude as the best CNT/PPy fibers with the added benefit of solution processing. The conductivity and mechanical properties of these fibers depended greatly on the processing conditions such as the polymerization rate. Faster rates led to conductive polymer films of lower uniformity and lower conductivity. Since a fast polymerization rate was needed to stabilize these fibers, they would inherently produce fibers with conductive polymer films that have many nucleation sites. This led to rough films with cracks. This was likely the cause of the brittle nature found for all of the fibers. Another cause could be the layering of conductive polymer in the fibers. These layers may not interact strongly, allowing cracks in the conductive polymer surface to propagate through the fiber. Because of these difficulties, quantitative measurements of the strengths of these fibers could not be accomplished. The conditions leading to semicontinuous fiber formation are summarized in Table 2.

**Table 2. Summary of CNT Dispersion and Oxidant Solution Conditions and the Resulting Fibers**

| CNT dispersion | oxidant solution | fiber formation | max conductivity (S/cm) |
|---|---|---|---|
| SWNT/P3HT/PPy (1/1/4) | 0.5 M $FeCl_3$ in ethanol | none | |
| SWNT/P3HT/PPy (1/1/400) | 0.5 M $FeCl_3$ in ethanol | none | |
| SWNT/P3HT/PPy (1/1/40) | 0.05 M $FeCl_3$ in ethanol | none | |
| | 0.5 M $FeCl_3$ in ethanol | semicontinuous | 170 |
| | 5 M $FeCl_3$ in ethanol | discontinuous | 3 |
| | 0.5 M $FeCl_3$ + phytic acid in ethanol | semicontinuous | 19 |
| SWNT/P3HT/EDOT (1/1/40) | 0.5 M $FeCl_3$ in ethanol | discontinuous | 7 |
| | 0.5 M $FeCl_3$ + phytic acid in ethanol | semicontinuous | 64 |

## CONCLUSIONS

Solution-processed, conductive SWNT/conjugated polymer composite films and fibers were formed using in-situ polymerization of conductive polymer. In-situ polymerization increased the processability of the SWNT/conjugated polymer gels allowing for production of transparent electrodes as well as composite fibers. The oxidant, $FeCl_3$, doped both the polymer and the SWNTs, leading to highly conductive composites. The films reached conductivities of 2800 and 3300 S/cm for SWNT/P3HT/PPy and SWNT/P3HT/PEDOT composites, respectively. These films open up the possibility of using SWNT/conjugated polymer films as solution-processable transparent electrodes. The fibers reach conductivities of up to 170 S/cm. Two fiber-forming regimes were found, which depended on the extrusion rate of the fiber. Phytic acid was needed as a noncovalent cross-linker to strengthen the fibers. All additives needed to make conductive films and fibers are inexpensive or at low concentrations, which enables large-scale processing. These results show that in-situ polymerization of conductive polymer can be a promising tool in solution-processed manufacturing.

## ASSOCIATED CONTENT

### Supporting Information

SEM images of SWNT/P3HT/PEDOT films, gel fibers made without additional polymerization of conductive polymer, development of fiber processing, SEM images of fibers with excess $FeCl_3$, details on the variables tested during fiber optimization, and energy-dispersive X-ray spectroscopy and thermogravimetric analysis of various fibers are analyzed. This material is available free of charge via the Internet at http://pubs.acs.org.

## AUTHOR INFORMATION

### Corresponding Author

*E-mail: zbao@stanford.edu.

### Notes

The authors declare no competing financial interest.

## ACKNOWLEDGMENTS

We thank the Center for Advanced Molecular Photovoltaics (CAMP) and Global Climate and Energy Project (GCEP) at

Stanford University and the Stanford Graduate Fellowship for funding this project.

## REFERENCES

(1) Hammock, M. L.; Chortos, A.; Tee, B. C. K.; Tok, J. B. H.; Bao, Z. 25th Anniversary Article: The Evolution of Electronic Skin (E-Skin): A Brief History, Design Considerations, and Recent Progress. *Adv. Mater.* **2013**, *25*, 5997−6038.
(2) Sokolov, A. N.; Tee, B. C. K.; Bettinger, C. J.; Tok, J. B. H.; Bao, Z. Chemical and Engineering Approaches to Enable Organic Field-Effect Transistors for Electronic Skin Applications. *Acc. Chem. Res.* **2011**, *45*, 361−371.
(3) Pan, L.; Chortos, A.; Yu, G.; Wang, Y.; Isaacson, S.; Allen, R.; Shi, Y.; Dauskardt, R.; Bao, Z. An Ultra-Sensitive Resistive Pressure Sensor Based on Hollow-Sphere Microstructure Induced Elasticity in Conducting Polymer Film. *Nat. Commun.* **2014**, *5*, 3002.1−3002.8.
(4) Hecht, D. S.; Hu, L.; Irvin, G. Emerging Transparent Electrodes Based on Thin Films of Carbon Nanotubes, Graphene, and Metallic Nanostructures. *Adv. Mater.* **2011**, *23*, 1482−1513.
(5) Lipomi, D. J.; Vosgueritchian, M.; Tee, B. C. K.; Hellstrom, S. L.; Lee, J. A.; Fox, C. H.; Bao, Z. Skin-Like Pressure and Strain Sensors Based on Transparent Elastic Films of Carbon Nanotubes. *Nat. Nanotechnol.* **2011**, *6*, 788−792.
(6) Hecht, D.; Hu, L.; Gruner, G. Conductivity Scaling with Bundle Length and Diameter in Single Walled Carbon Nanotube Networks. *Appl. Phys. Lett.* **2006**, *89*, 133112.1−133112.3.
(7) De, S.; Lyons, P. E.; Sorel, S.; Doherty, E. M.; King, P. J.; Blau, W. J.; Nirmalraj, P. N.; Boland, J. J.; Scardaci, V.; Joimel, J.; Coleman, J. N. Transparent, Flexible, and Highly Conductive Thin Films Based on Polymer−Nanotube Composites. *ACS Nano* **2009**, *3*, 714−720.
(8) Weng, Y.-T.; Wu, N.-L. N. Fabrication of Graphite Oxide/Pedot-Pss/Carbon Nanotubes Composite Paper Via One Step Solution-Casting Synthesis for High Performance Flexible Electrode. *Electrochem. Soc. Meeting Abstr.* **2012**, *2*, 585−585.
(9) Wang, K.; Meng, Q.; Zhang, Y.; Wei, Z.; Miao, M. High-Performance Two-Ply Yarn Supercapacitors Based on Carbon Nanotubes and Polyaniline Nanowire Arrays. *Adv. Mater.* **2013**, *25*, 1494−1498.
(10) Ren, J.; Li, L.; Chen, C.; Chen, X.; Cai, Z.; Qiu, L.; Wang, Y.; Zhu, X.; Peng, H. Twisting Carbon Nanotube Fibers for Both Wire-Shaped Micro-Supercapacitor and Micro-Battery. *Adv. Mater.* **2013**, *25*, 1155−1159.
(11) Bai, X.; Hu, X.; Zhou, S.; Yan, J.; Sun, C.; Chen, P.; Li, L. In Situ Polymerization and Characterization of Grafted Poly (3,4-Ethylenedioxythiophene)/Multiwalled Carbon Nanotubes Composite with High Electrochemical Performances. *Electrochim. Acta* **2013**, *87*, 394−400.
(12) Baughman, R. H. Playing Nature's Game with Artificial Muscles. *Science* **2005**, *308*, 63−65.
(13) Tissaphern, M.; Jiyoung, O.; Mikhail, K.; Eddie Chi Wah, F.; Mei, Z.; Shaoli, F.; Ray, H. B.; John, D. W. M. Electrochemical Actuation of Carbon Nanotube Yarns. *Smart Mater. Struct.* **2007**, *16*, S243−S249.
(14) Zhang, M.; Atkinson, K. R.; Baughman, R. H. Multifunctional Carbon Nanotube Yarns by Downsizing an Ancient Technology. *Science* **2004**, *306*, 1358−1361.
(15) Wang, X.; Yong, Z. Z.; Li, Q. W.; Bradford, P. D.; Liu, W.; Tucker, D. S.; Cai, W.; Wang, H.; Yuan, F. G.; Zhu, Y. T. Ultrastrong, Stiff and Multifunctional Carbon Nanotube Composites. *Mater. Res. Lett.* **2013**, *1*, 1−7.
(16) Koziol, K.; Vilatela, J.; Moisala, A.; Motta, M.; Cunniff, P.; Sennett, M.; Windle, A. High-Performance Carbon Nanotube Fiber. *Science* **2007**, *318*, 1892−1895.
(17) Ma, W.; Liu, L.; Zhang, Z.; Yang, R.; Liu, G.; Zhang, T.; An, X.; Yi, X.; Ren, Y.; Niu, Z.; Li, J.; Dong, H.; Zhou, W.; Ajayan, P. M.; Xie, S. High-Strength Composite Fibers: Realizing True Potential of Carbon Nanotubes in Polymer Matrix through Continuous Reticulate Architecture and Molecular Level Couplings. *Nano Lett.* **2009**, *9*, 2855−2861.
(18) Chae, H. G.; Minus, M. L.; Rasheed, A.; Kumar, S. Stabilization and Carbonization of Gel Spun Polyacrylonitrile/Single Wall Carbon Nanotube Composite Fibers. *Polymer* **2007**, *48*, 3781−3789.
(19) Ko, F.; Gogotsi, Y.; Ali, A.; Naguib, N.; Ye, H.; Yang, G.; Li, C.; Willis, P. Electrospinning of Continuous Carbon Nanotube-Filled Nanofiber Yarns. *Adv. Mater.* **2003**, *15*, 1161−1165.
(20) Jalili, R.; Razal, J. M.; Wallace, G. G. Wet-Spinning of Pedot:Pss/Functionalized-Swnts Composite: A Facile Route toward Production of Strong and Highly Conducting Multifunctional Fibers. *Sci. Rep.* **2013**, *3*, 3438.1−3438.7.
(21) Davis, V. A.; Parra-Vasquez, A. N. G.; Green, M. J.; Rai, P. K.; Behabtu, N.; Prieto, V.; Booker, R. D.; Schmidt, J.; Kesselman, E.; Zhou, W.; Fan, H.; Adams, W. W.; Hauge, R. H.; Fischer, J. E.; Cohen, Y.; Talmon, Y.; Smalley, R. E.; Pasquali, M. True Solutions of Single-Walled Carbon Nanotubes for Assembly into Macroscopic Materials. *Nat. Nanotechnol.* **2009**, *4*, 830−834.
(22) Chou, T.-W.; Gao, L.; Thostenson, E. T.; Zhang, Z.; Byun, J.-H. An Assessment of the Science and Technology of Carbon Nanotube-Based Fibers and Composites. *Compos. Sci. Technol.* **2010**, *70*, 1−19.
(23) Vigolo, B.; Pénicaud, A.; Coulon, C.; Sauder, C.; Pailler, R.; Journet, C.; Bernier, P.; Poulin, P. Macroscopic Fibers and Ribbons of Oriented Carbon Nanotubes. *Science* **2000**, *290*, 1331−1334.
(24) Allen, R.; Fuller, G. G.; Bao, Z. Aligned Swnt Films from Low-Yield Stress Gels and Their Transparent Electrode Performance. *ACS Appl. Mater. Interfaces* **2013**, *5*, 7244−7252.
(25) Allen, R.; Bao, Z.; Fuller, G. G. Oriented, Polymer-Stabilized Carbon Nanotube Films: Influence of Dispersion Rheology. *Nanotechnology* **2013**, *24*, 015709.
(26) Lee, H. W.; You, W.; Barman, S.; Hellstrom, S.; LeMieux, M. C.; Oh, J. H.; Liu, S.; Fujiwara, T.; Wang, W. M.; Chen, B.; Jin, Y. W.; Kim, J. M.; Bao, Z. Lyotropic Liquid-Crystalline Solutions of High-Concentration Dispersions of Single-Walled Carbon Nanotubes with Conjugated Polymers. *Small* **2009**, *5*, 1019−1024.
(27) Topsoe, H. Geometric Factors in Four Point Resistivity Measurement. *Bridge Technol.* **1968**, *472−13*, 58−59.
(28) Schroder, D. K. *Semiconductor Material and Device Characterization*, 3rd ed.; John Wiley & Sons: Hoboken, NJ, 2006.
(29) Zhou, J.; Lubineau, G. Improving Electrical Conductivity in Polycarbonate Nanocomposites Using Highly Conductive Pedot/Pss Coated Mwcnts. *ACS Appl. Mater. Interfaces* **2013**, *5*, 6189−6200.
(30) Kumar, A.; Zhou, C. The Race to Replace Tin-Doped Indium Oxide: Which Material Will Win? *ACS Nano* **2010**, *4*, 11−14.
(31) Chen, X.; Inganäs, O. Three-Step Redox in Polythiophenes: Evidence from Electrochemistry at an Ultramicroelectrode. *J. Phys. Chem.* **1996**, *100*, 15202−15206.
(32) Damlin, P.; Kvarnström, C.; Ivaska, A. Electrochemical Synthesis and in Situ Spectroelectrochemical Characterization of Poly(3,4-Ethylenedioxythiophene) (Pedot) in Room Temperature Ionic Liquids. *J. Electroanal. Chem.* **2004**, *570*, 113−122.
(33) Guerini, S.; Filho, A. G. S.; Filho, J. M.; Alves, O. L.; Fagan, S. B. Electronic Properties of Fecl_{3}-Adsorbed Single-Wall Carbon Nanotubes. *Phys. Rev. B* **2005**, *72*, 233401.1−233401.4.
(34) De Blauwe, K.; Kramberger, C.; Plank, W.; Kataura, H.; Pichler, T. Raman Response of Fecl3 Intercalated Single-Wall Carbon Nanotubes at High Doping. *Phys. Status Solidi B* **2009**, *246*, 2732−2736.
(35) Tat'yana, V. V.; Oleg, N. E. Polypyrrole: A Conducting Polymer; Its Synthesis, Properties and Applications. *Russ. Chem. Rev.* **1997**, *66*, 443−457.
(36) Wang, X.-S.; Tang, H.-P.; Li, X.-D.; Hua, X. Investigations on the Mechanical Properties of Conducting Polymer Coating-Substrate Structures and Their Influencing Factors. *Int. J. Mol. Sci.* **2009**, *10*, 5257−5284.
(37) O'Connor, B.; Chan, E. P.; Chan, C.; Conrad, B. R.; Richter, L. J.; Kline, R. J.; Heeney, M.; McCulloch, I.; Soles, C. L.; DeLongchamp, D. M. Correlations between Mechanical and Electrical Properties of Polythiophenes. *ACS Nano* **2010**, *4*, 7538−7544.
(38) Foroughi, J.; Ghorbani, S. R.; Peleckis, G.; Spinks, G. M.; Wallace, G. G.; Wang, X. L.; Dou, S. X. The Mechanical and the

Electrical Properties of Conducting Polypyrrole Fibers. *J. Appl. Phys.* **2010**, *107*, 103712.1−103712.4.
(39) Pan, L.; Yu, G.; Zhai, D.; Lee, H. R.; Zhao, W.; Liu, N.; Wang, H.; Tee, B. C.-K.; Shi, Y.; Cui, Y.; Bao, Z. Hierarchical Nanostructured Conducting Polymer Hydrogel with High Electrochemical Activity. *Proc. Natl. Acad. Sci. U.S.A.* **2012**, *109*, 9287−9292.
(40) Kim, Y. H.; Sachse, C.; Machala, M. L.; May, C.; Müller-Meskamp, L.; Leo, K. Highly Conductive Pedot:Pss Electrode with Optimized Solvent and Thermal Post-Treatment for Ito-Free Organic Solar Cells. *Adv. Funct. Mater.* **2011**, *21*, 1076−1081.
(41) Chen, M.; Guthy, C.; Vavro, J.; Fischer, J. E.; Badaire, S.; Zakri, C.; Poulin, P.; Pichot, V.; Launois, P. Characterization of Single-Walled Carbon Nanotube Fibers and Correlation with Stretch Alignment. *Mater. Res. Soc. Symp. Proc.* **2005**, *858E*, HH4.11.1−HH4.11.6.
(42) Foroughi, J.; Spinks, G. M.; Ghorbani, S. R.; Kozlov, M. E.; Safaei, F.; Peleckis, G.; Wallace, G. G.; Baughman, R. H. Preparation and Characterization of Hybrid Conducting Polymer−Carbon Nanotube Yarn. *Nanoscale* **2012**, *4*, 940−945.